ACS APPLIED MATERIALS & INTERFACES

www.acsami.org

Research Article

Bioelectrocatalytic CO_2 Reduction by Redox Polymer-Wired Carbon Monoxide Dehydrogenase Gas Diffusion Electrodes

Jana M. Becker, Anna Lielpetere, Julian Szczesny, João R. C. Junqueira, Patricia Rodríguez-Maciá, James A. Birrell, Felipe Conzuelo,* and Wolfgang Schuhmann*

Cite This: *ACS Appl. Mater. Interfaces* 2022, 14, 46421−46426

Read Online

ACCESS | Metrics & More | Article Recommendations | Supporting Information

ABSTRACT: The development of electrodes for efficient CO_2 reduction while forming valuable compounds is critical. The use of enzymes as catalysts provides the advantage of high catalytic activity in combination with highly selective transformations. We describe the electrical wiring of a carbon monoxide dehydrogenase II from *Carboxydothermus hydrogenoformans* (*Ch*CODH II) using a cobaltocene-based low-potential redox polymer for the selective reduction of CO_2 to CO over gas diffusion electrodes. High catalytic current densities of up to −5.5 mA cm^{-2} are achieved, exceeding the performance of previously reported bioelectrodes for CO_2 reduction based on either carbon monoxide dehydrogenases or formate dehydrogenases. The proposed bioelectrode reveals considerable stability with a half-life of more than 20 h of continuous operation. Product quantification using gas chromatography confirmed the selective transformation of CO_2 into CO without any parasitic co-reactions at the applied potentials.

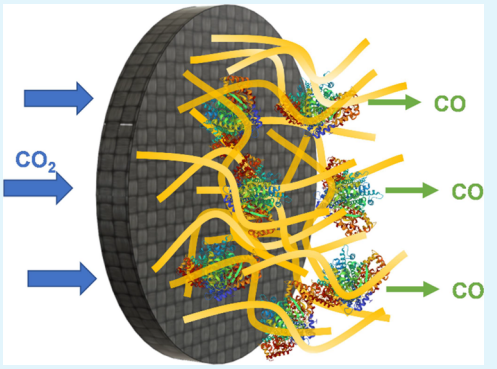

KEYWORDS: *carbon monoxide dehydrogenase, CO_2 reduction, enzymes, gas diffusion electrodes, redox polymers*

INTRODUCTION

As a greenhouse gas, increasing amounts of CO_2 in the atmosphere contribute significantly to climate change.[1] The reduction of CO_2 has become of significant importance over the course of the last few years, as it offers the possibility to decrease the amounts of CO_2 present in the atmosphere. Furthermore, it allows for the use of CO_2 as an alternative carbon feedstock to fossil fuels.[2] Due to the inert nature of CO_2, an efficient catalyst is crucial to reducing CO_2 for the synthesis of valuable products. So far, substantial research has been put into using abiotic catalysts, such as metals, metal oxides, N-doped carbon materials, and molecular catalysts for electrocatalytic CO_2 reduction.[3−7] However, these catalysts are commonly operated under harsh conditions and often suffer from low product specificity due to the competing H_2 evolution reaction. Therefore, considerable efforts are needed for the design and operation of catalysts providing high conversion selectivities.[8] The ability of enzymes to effectively catalyze reactions toward specific products in aqueous electrolytes at mild pH and temperature makes them highly advantageous catalysts to be investigated.[9] Recently, several studies have been devoted to the characterization and potential applications of the only two enzymes capable of directly reducing CO_2 to CO and formate, namely, carbon monoxide dehydrogenase and formate dehydrogenase, respectively.[10]

Carbon monoxide dehydrogenases (CODHs) are highly active and efficient enzymes known to catalyze the conversion between CO and CO_2.[11] Among the different enzyme classes, Mo/Cu-containing CODHs are air-stable but only capable of the unidirectional oxidation of CO to CO_2.[12] In contrast, the Ni-containing CODHs are extremely oxygen sensitive[13] but allow for bidirectional reversible catalysis (see eq 1) and thereby are suited for CO_2 reduction. The active site, containing a [$NiFe_4S_4$] cluster, possesses at least three different redox states. Two of these redox states, C_{red1} and C_{red2}, are thought to take part in the catalytic cycle.[13−16] It is assumed that CO_2 binds to the Ni ion in the C_{red2} state, via the carbon in a bent configuration where one of the oxygens interacts with a dangler iron ion and the other is stabilized by hydrogen bonds from the protein environment.[15] The [3Fe−4S−Ni] part of the C-cluster is thought to transfer two electrons to CO_2, while the dangler iron facilitates C−O bond cleavage and hydroxide formation.[13] The redox states interconvert with an average redox potential of $E(C_{red1}/C_{red2})$ = −530 mV vs SHE, very close to the thermodynamic potential for the CO_2/CO couple at pH 7.[13,16] Additionally, an inactive oxidized state of the enzyme (C_{ox}) can form at potentials more positive than −300 mV vs SHE.[13] Thus, the enzyme can be inactivated by exposure to high potentials.[17]

Received: May 28, 2022
Accepted: September 13, 2022
Published: October 4, 2022

$$CO_2 + 2H^+ + 2e^- \leftrightarrows CO + H_2O \quad (1)$$

Recent reports have shown the fabrication of highly active bioelectrodes for CO_2 reduction using a recombinant CODH from *Rhodospirillum rubrum* in direct electron transfer (DET) with carbon nanotube-modified electrode surfaces.[16,18] Although the current densities of these electrodes reached up to −4.9 mA cm^{-2},[18] approaching the performance of metal- and molecular-based catalysts,[16] the use of specific linkers for adequate enzyme immobilization was crucial for optimum performance. Under DET configuration, the enzymes must be in direct contact with the electrode and in an appropriate orientation to allow electrical wiring to the conductive surface.[19] In contrast, the use of redox mediators to shuttle electrons between enzymes and the electrode provides effective electron transfer independent of the biomolecule orientation and with the possibility to wire more enzymes than only those in direct contact with the electrode surface. Such a mediated electron transfer configuration has been demonstrated for a CODH from *Moorella thermoacetica* in solution using methyl viologen as the redox mediator.[20] However, the use of freely diffusing redox mediators has the disadvantage of potential mediator leakage, limiting the long-term stability of the electrode.[21] Furthermore, it can lead to short-circuiting in a complete electrolyzer. In that respect, redox polymers are advantageous for the fabrication of bioelectrodes due to the covalent tethering of the redox moieties to a polymer backbone. In addition, the three-dimensional polymeric matrix is beneficial for the stable entrapment of enzymes on the electrode surface, allowing immobilization and electrical wiring of an increased number of enzyme molecules.[22]

Here, we present the electrical wiring of CODH II from *Carboxydothermus hydrogenoformans* using a low-potential redox polymer, constituting the first report on the integration of a CODH within a redox hydrogel. A cobaltocene derivative bound to branched polyethylenimine (BPEI-[$CoCp_2$])[23,24] is employed for enzyme immobilization and electrical wiring with the electrode surface enabling the fabrication of efficient gas diffusion bioelectrodes for bioelectrocatalytic CO_2 reduction.

RESULTS AND DISCUSSION

For the development of the CODH-based CO_2-reducing bioelectrode, a gas diffusion layer was used as the electrode substrate. Gas diffusion electrodes circumvent mass transport limitations by decreasing the diffusional pathways of gaseous substrates and therefore increasing the flux of substrate toward the catalytic sites, which results in an increased catalytic current.[25] This strategy has been demonstrated for the fabrication of bioelectrodes integrating isolated enzymes within redox polymer matrices for the highly efficient conversion of gaseous substrates such as H_2[26−28] and CO_2.[29]

The carbon-based gas diffusion electrode was first modified by means of electrografting, leading to a monolayer of free amino groups on the electrode surface to attain an adequate stability of the modification layer. Then, the electrode was modified with a mixture of the redox polymer BPEI-[$CoCp_2$] and the isolated enzyme *Ch*CODH II. To attach the film covalently to the electrode surface and generate a cross-linked three-dimensional network entrapping the enzyme over the electrode, the crosslinker poly(ethylene glycol) diglycidyl ether (PEGDGE) was added. Figure 1 depicts a schematic representation of the modified electrode.

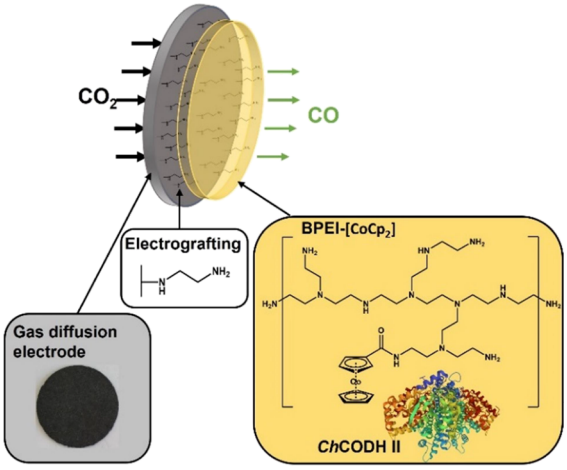

Figure 1. Schematic representation of the redox polymer/enzyme gas diffusion electrode for CO_2 reduction. The image includes an optical micrograph of the modified gas diffusion electrode, the electrografted layer of ethylenediamine, the structures of the redox polymer BPEI-[$CoCp_2$], and the enzyme CODH II from *C. hydrogenoformans* (*Ch*CODH II, PDB ID: 1SUF[30,31]).

We first evaluated the ability of the redox polymer to wire CODH to the electrode. The cobaltocene-based redox polymer deposited on a glassy carbon electrode in the absence of enzyme (Figure S1) revealed a midpoint potential of about −620 mV vs SHE. This midpoint potential was more negative than that of the enzyme $E(C_{red1}/C_{red2})$, ensuring adequate wiring for biocatalytic reduction processes. The modified electrodes integrating *Ch*CODH II were characterized using cyclic voltammetry in the absence and presence of CO_2. The cyclic voltammograms (CVs), displayed in Figure 2a, show a pronounced catalytic current in the presence of CO_2, while under an Ar atmosphere, only the response of the redox polymer can be seen. The current under turnover conditions reached up to −1.1 mA at an applied potential of −0.79 V vs SHE. This current accounts for a maximum current density of up to −5.5 mA cm^{-2} considering a geometric surface area of 0.2 cm^2. The difference between cathodic currents recorded under CO_2 and Ar at an applied potential of −0.79 V vs SHE was calculated to specifically determine the catalytic current density for CO_2 reduction, which amounted to −4.4 mA cm^{-2} (Figure 2b). The attained performance exceeds any previous reports on enzymatic CO_2 reduction, making use of either CODH or formate dehydrogenase with the enzyme in the DET regime or wired by redox mediators (see Table S1). A potential of −0.79 V vs SHE was chosen to examine the catalytic current since thereby a fully reduced redox polymer was ensured. However, more negative applied potentials were prevented to avoid interferences from reductive background processes taking place at the modified electrode. A control electrode was fabricated following the same modification approach but without integrating the CODH enzyme. Even at more negative applied potentials, no catalytic current response could be observed in the presence of CO_2 (Figure S2), confirming that the conversion was catalyzed by the enzyme.

The reaction products were quantified using gas chromatography to determine the selectivity and assess if other products were formed directly at the electrode or the redox polymer at the applied negative potentials. The gas diffusion cell was coupled to a gas chromatograph for in-line analysis of gaseous

https://doi.org/10.1021/acsami.2c09547
ACS Appl. Mater. Interfaces 2022, 14, 46421−46426

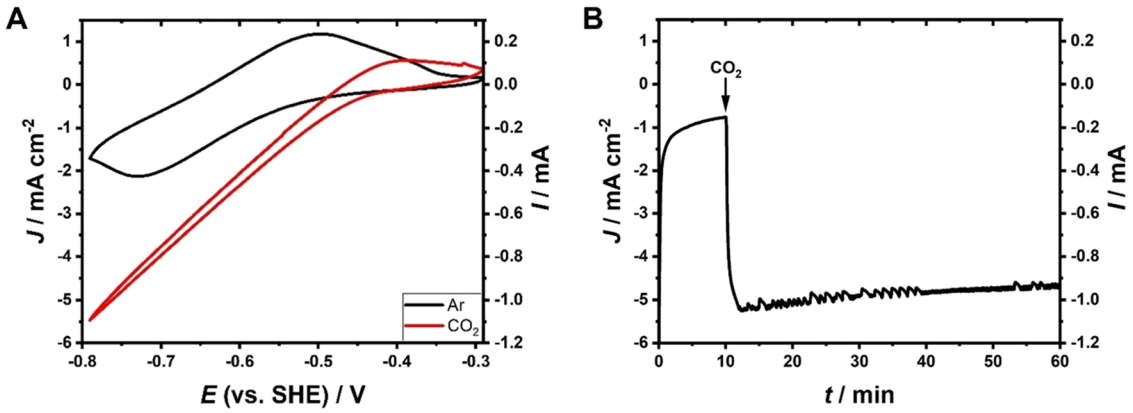

Figure 2. Electrochemical characterization using (A) cyclic voltammetry and (B) amperometry of a BPEI-[$CoCp_2$]/*Ch*CODH II-modified gas diffusion electrode using Ar or CO_2 applied to the backside of the electrode. Electrolyte: Ar-saturated 0.1 M phosphate buffer (pH 7.3). Scan rate in (A): 5 mV s^{-1}. Applied potential in (B): −0.79 V vs SHE. Current densities were calculated with respect to the modified geometric surface area (d = 5 mm).

product species during electrochemical measurements (Figure S3).

The analysis of a BPEI-[$CoCp_2$]/*Ch*CODH II-modified electrode at a constant applied potential of −0.79 V vs SHE with CO_2 provided to the backside of the electrode revealed the specific reduction of CO_2 to CO. CO, the expected product from the enzymatic conversion, was solely obtained with a Faradaic efficiency to be (82.1 ± 0.8)% (Figure 3; n = 3), while no other side products were observed (Figure S4). The samples for the analysis were only taken from the gaseous stream passing the backside of the electrode (see Figure S3), since CO exhibits a low solubility in aqueous solutions and will hence predominantly diffuse back to the gas phase from the three-phase reaction zone within the gas diffusion electrode.

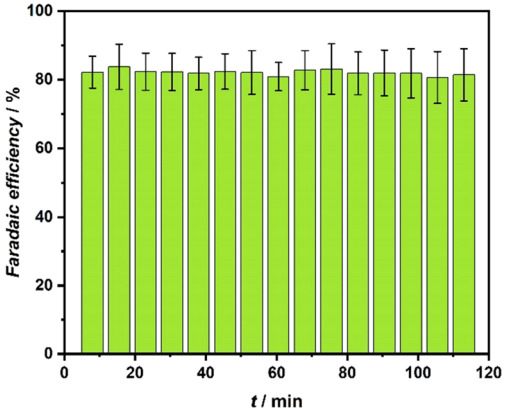

Figure 3. Faradaic efficiency calculated for the conversion of CO_2 with a BPEI-[$CoCp_2$]/*Ch*CODH II-modified electrode. The bioelectrode was operated under constant turnover conditions (CO_2, E_{app} = −0.79 V vs SHE) in Ar-saturated 0.1 M phosphate buffer (pH 7.3). Error bars represent the standard deviation (n = 3).

A BPEI-[$CoCp_2$]-modified control electrode without enzyme was analyzed at different applied potentials in the presence of CO_2 provided to the backside of the gas diffusion electrode. No products could be detected at any of the applied potentials (Figure S5), confirming that unspecific conversion of CO_2 or the formation of side products such as H_2 at the carbon-based gas diffusion electrode material or the redox polymer is negligible. The current observed during this measurement indicates that the remaining faradaic efficiency could be ascribed to background processes that are not related to enzymatic CO_2 conversion nor hydrogen evolution. The electrode could be safely operated at applied potentials as low as −0.79 V vs SHE where high catalytic currents were observed.

The stability of the modified bioelectrode under continuous turnover conditions was evaluated by means of amperometry at constant applied potentials (Figure 4). For the first 10 min,

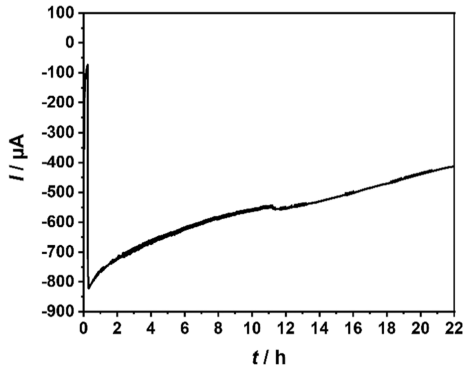

Figure 4. Stability measurement under continuous turnover conditions with a BPEI-[$CoCp_2$]/*Ch*CODH II-modified gas diffusion electrode. E_{app} = −0.79 V vs SHE. Electrolyte: Ar-saturated 0.1 M phosphate buffer (pH 7.3).

Ar was provided to the backside of the gas diffusion electrode to determine the background current before changing the gas feed to CO_2. The initial catalytic current was −0.75 mA, corresponding to a maximum turnover frequency of 2.7 s^{-1}. The amperometric measurement was run until the catalytic current had reached 50% of the initial catalytic current after 22 h. Although promising stability under continuous turnover was observed, the decrease in activity over time was likely due to an instability of the redox polymer film, as confirmed by a comparison of CVs recorded before and after the long-term catalytic conversion experiment (Figure S6).

CONCLUSIONS

To conclude, we report the successful wiring of the enzyme CODH II from *C. hydrogenoformans* on gas diffusion electrodes using the low potential redox polymer BPEI-[$CoCp_2$]. Product

https://doi.org/10.1021/acsami.2c09547
ACS Appl. Mater. Interfaces 2022, 14, 46421−46426

analysis via GC confirmed selective enzymatic CO_2 conversion to CO without the formation of any side products at negative applied potentials. The outstanding performance of the fabricated bioelectrode in terms of achieved current densities and operational stability highlights the potential of redox enzymes for the fabrication of functional CO_2-electroreduction systems. Based on the developed bioelectrode, the synthesis of products with a higher value is envisaged by the establishment of catalytic cascade reaction systems.

EXPERIMENTAL SECTION

Chemicals and Materials. All chemicals (reagent or higher grade) were purchased from Sigma Aldrich, Merck, VWR, or Fisher Scientific and were used as received. The cobaltocene precursor was purchased from MCAT. Carbon dioxide (≥99.9%) was from Air Liquide. Distilled water was obtained using a Millipore water purification system.

Enzyme Expression and Purification. A gene encoding CODH II (AF249899.1) from *Carboxydothermus hydrogenoformans* strain Z-2901 was ordered from GenScript as a codon-optimized DNA sequence in pUC57 containing KasI and PstI restriction sites at the 5′ and 3′ ends, respectively. The *Ch*CODH II gene was subcloned into the expression plasmid pASK-IBA17+ between the KasI and PstI sites giving a construct that encodes *Ch*CODH II with an amino-terminal Strep-tag II and TEV protease cleavage site. BL21(DE3) Δ*iscR* cells[1] were transformed with the *Ch*CODH II construct and grown at 37 °C in LB-phosphate containing 0.5% (w/v) glucose, 1 mM $NiCl_2$, 2 mM ammonium iron citrate, 5 mM L-cysteine, 100 μg mL^{-1} ampicillin, and 50 μg mL^{-1} kanamycin to an optical density of 0.6 at 600 nm. The cell suspension was then transferred to sealed bottles and purged with N_2 before protein production was induced by addition of 200 μg L^{-1} anhydrotetracycline overnight at room temperature. Cells were harvested by centrifugation, resuspended in 100 mM Tris−HCl, 150 mM NaCl, pH 8, and lysed by sonication. The cell suspension was clarified by centrifugation, and the protein was purified from the supernatant using a Streptactin column (IBA). The purified protein was concentrated to 486 μM, sealed in glass vials, and stored at −80 °C until use.

Redox Polymer Synthesis. BPEI (40 mg, 50 wt % in water) was dried overnight in a vacuum. Then, 20 mg of the dried polymer backbone was dissolved in dry dimethyl sulfoxide (DMSO) (1.3 mL) under an Ar atmosphere and fresh Ar-saturated Et_3N (12 μL) was added. The solution was stirred for 5 min. Three vacuum-Ar cycles were carried out to ensure completely O_2-free conditions. The redox mediator 1-(2,5-dioxopyrrolidinylcarboxy)-cobaltocenium hexafluorophosphate (12 mg) was dissolved in dry DMSO (1 mL). Then, the yellow mediator containing solution was slowly added to the BPEI solution and the whole mixture was stirred overnight (20 h) under an Ar atmosphere at 28 °C. Afterward, Et_2O (10 mL) was added, which leads to the precipitation of a dark yellow oil. Et_2O was added additionally two times (10 mL each) until the solution was colorless. Thereafter, the crude product sample was washed first with CH_2Cl_2 (10 mL) and second using MeOH (10 mL). The residue was left to dry under vacuum for two nights. The dried polymer was resolubilized in H_2O (2 mL) leading to a polymer concentration of 7.0 mg mL^{-1}.

Electrode Preparation. The electrode material was first modified by means of an electrografting procedure using a μAutolab Type III potentiostat. A carbon-based gas diffusion layer (H23, Freudenberg Performance Materials; 210 μm thickness, d = 1.8 cm), used as an electrode substrate, was fixed in a cell exposing a defined electrode area and only one side of the electrode surface for modification. Then, cyclic voltammetry in a range from 0.0 to 1.4 V vs pseudo-Ag/AgCl reference electrode at a scan rate of 50 mV s^{-1} for 20 cycles was performed in 15 mM *N*-Boc-ethylenediamine and 0.15 M $TBABF_4$ in MeCN. Afterward, the electrode was rinsed with EtOH. For deprotection of the *N*-Boc-protected amino groups, the electrode was treated with 4 M HCl in dioxane for at least 1 h. Then, the electrode was submerged in EtOH (2 min) and then washed with H_2O. After drying under ambient conditions, the electrode was transferred into an anaerobic glovebox for the modification with the catalytically active layer. A solution of BPEI-[$CoCp_2$] (20 μL, 7.0 mg mL^{-1}), CODH (3 μL, 486 μM), and PEGDGE (4 μL, 1:40 dilution in H_2O) was deposited over the electrode surface by means of drop-casting, modifying an area of 0.2 cm^2, and left to dry overnight in the anaerobic glovebox before being used for electrochemical measurements. For control experiments, the electrode was modified only with BPEI-[$CoCp_2$] (15.4 μL, 13.5 mg mL^{-1}) and PEGDGE (4.62 μL, 1:40 dilution in H_2O). An electrode modified with BPEI-[$CoCp_2$] (20 μL, 7.0 mg mL^{-1}) and PEGDGE (4 μL, 1:40 dilution in H_2O) was used for the control experiment with in-line coupled gas chromatography. The gas diffusion cell was assembled inside the glovebox. To avoid leakage of electrolyte through the hydrophilized electrode, an H23I2 gas diffusion layer (Freudenberg Performance Materials, 210 μm thickness, d = 1.8 cm) with an additional hydrophobic treatment was positioned behind the modified electrode. For the electrochemical measurements, the cell was taken out of the glovebox but kept under an Ar atmosphere.

For the characterization of the low potential redox polymer, a glassy carbon electrode was modified with BPEI-[$CoCp_2$] (3 μL, 7.0 mg mL^{-1}) and let to dry under ambient conditions.

Electrochemical Measurements. All electrochemical measurements were performed in a standard three-electrode setup, employing a gas diffusion cell.[2] The enzyme-modified electrode acted as the working electrode. An Ag/AgCl/3 M KCl reference electrode and a Pt wire counter electrode were employed. A Gamry Reference 1000 potentiostat was used for all electrochemical measurements. The potentials are given vs the standard hydrogen electrode (SHE) according to $E_{SHE} = E_{Ag/AgCl/3\ M\ KCl} + 210$ mV. The reported current densities were calculated regarding the modified geometric surface area of the electrode (A = 0.2 cm^2). The experiments were conducted outside of the glovebox under anaerobic conditions by purging the buffer continuously with Ar while providing either Ar or CO_2 to the backside of the gas-diffusion electrode. To adjust to the different gas feeds to the backside of the electrode between measurements, the electrodes were exposed for 5 min to the corresponding gas feed before starting the measurement. As electrolyte, 0.1 M phosphate buffer with a pH value of 7.3 was used.

The modified gas diffusion electrodes were electrochemically characterized by means of cyclic voltammetry in a potential range between −0.29 and −0.79 V vs SHE at a scan rate of 5 mV s^{-1}. The long-term stability of the fabricated bioelectrode was evaluated using amperometry at a constant applied potential of −0.79 V vs SHE. To determine the background current, the first 10 min of the chronoamperometric measurement was recorded under Ar flow before switching to CO_2. For characterization of the redox polymer, the modified glassy carbon electrode was placed in a standard electrochemical cell. The measurement was conducted in Ar-purged 0.1 M phosphate buffer (pH 7.3) at a scan rate of 50 mV s^{-1}.

Gas Chromatography. To analyze the products formed during conversion, a three-electrode setup was used, with a Ag/AgCl/3 M KCl reference electrode and a stainless-steel canula counter electrode. The gas diffusion cell was coupled to a multiple gas analyzer #1 gas chromatograph (GC, SRI Instruments). The GC has a 3 m HayeSep D column and two detectors. A flame ionization detector equipped with a methanizer for the detection of CO and a thermal conductivity detector for the H_2 analysis were used. As the carrier gas, N_2 was used. The electrode was exposed to a constant flow of CO_2, controlled with a mass flow controller (AALBORG) to the backside of the electrode while applying a constant potential of −0.79 V vs SHE. A photograph of the cell can be seen in Figure S3. The gas phase at the backside of the electrode was directly injected into the GC. For control experiments, an electrode modified following the same fabrication procedure but in the absence of enzyme was used. A chronoamperometric measurement was performed to investigate the possible formation of side products by stepping the applied potential from −0.29 to −0.79 V vs SHE in steps of 100 mV. Each potential was applied for 15 min. An Autolab PGSTAT302N was used during electrochemical measurements coupled to GC detection. The faradaic

https://doi.org/10.1021/acsami.2c09547
ACS Appl. Mater. Interfaces 2022, 14, 46421−46426

efficiency (FE, %) was calculated according to eq 2,[3] with F = Faraday constant (96,485 C mol^{-1}), ne^- = number of electrons needed for the reduction reaction, nr(CO) = concentration of CO detected by GC (vol%), f = gas flow rate (L s^{-1}), V_m = molar volume of an ideal gas (22.4 L mol^{-1}), and I = measured current at the time of sampling:

$$\mathrm{FE} = \frac{F \times ne^- \frac{nr(\mathrm{CO}) \times f}{V_m}}{I} \times 100 \quad (2)$$

■ ASSOCIATED CONTENT

Supporting Information

The Supporting Information is available free of charge at https://pubs.acs.org/doi/10.1021/acsami.2c09547.

Literature comparison; redox polymer characterization; gas chromatography setup and results; and voltammetric characterization before and after long-term measurement (PDF)

■ AUTHOR INFORMATION

Corresponding Authors

Felipe Conzuelo − *Instituto de Tecnologia Química e Biológica António Xavier, Universidade Nova de Lisboa, 2780-157 Oeiras, Portugal*; Email: felipe.conzuelo@itqb.unl.pt

Wolfgang Schuhmann − *Analytical Chemistry—Center for Electrochemical Sciences (CES), Faculty of Chemistry and Biochemistry, Ruhr-Universität Bochum, D-44780 Bochum, Germany*; orcid.org/0000-0003-2916-5223; Email: wolfgang.schuhmann@rub.de

Authors

Jana M. Becker − *Analytical Chemistry—Center for Electrochemical Sciences (CES), Faculty of Chemistry and Biochemistry, Ruhr-Universität Bochum, D-44780 Bochum, Germany*

Anna Lielpetere − *Analytical Chemistry—Center for Electrochemical Sciences (CES), Faculty of Chemistry and Biochemistry, Ruhr-Universität Bochum, D-44780 Bochum, Germany*

Julian Szczesny − *Analytical Chemistry—Center for Electrochemical Sciences (CES), Faculty of Chemistry and Biochemistry, Ruhr-Universität Bochum, D-44780 Bochum, Germany*

João R. C. Junqueira − *Analytical Chemistry—Center for Electrochemical Sciences (CES), Faculty of Chemistry and Biochemistry, Ruhr-Universität Bochum, D-44780 Bochum, Germany*

Patricia Rodríguez-Maciá − *Department of Inorganic Spectroscopy, Max Planck Institute for Chemical Energy Conversion, D-45470 Mülheim an der Ruhr, Germany*; Present Address: Inorganic Chemistry Laboratory, Department of Chemistry, University of Oxford, South Parks Road, OX1 3QR Oxford, U.K; orcid.org/0000-0003-3513-0115

James A. Birrell − *Department of Inorganic Spectroscopy, Max Planck Institute for Chemical Energy Conversion, D-45470 Mülheim an der Ruhr, Germany*; orcid.org/0000-0002-0939-0573

Complete contact information is available at: https://pubs.acs.org/10.1021/acsami.2c09547

Notes

The authors declare no competing financial interest.

■ ACKNOWLEDGMENTS

The authors are grateful for financial support from the Deutsche Forschungsgemeinschaft (DFG, German Research Foundation) in the framework of the SPP2240 (e-biotech) [445820469] and the European Union's Horizon 2020 research and innovation program under the Marie Skłodowska-Curie MSCA-ITN "ImplantSens" [813006]. J.A.B. acknowledges funding from the DFG SPP 1927 "Iron−Sulfur for Life" project (Project No. BI 2198/1-1) and the Max Planck Society. P.R.-M. thanks the University of Oxford for a Glasstone Research Fellowship and Linacre College Oxford for a Junior Research Fellowship.

■ REFERENCES

(1) Solomon, S.; Plattner, G.-K.; Knutti, R.; Friedlingstein, P. Irreversible Climate Change due to Carbon Dioxide Emissions. *Proc. Natl. Acad. Sci. U. S. A.* **2009**, *106*, 1704−1709.

(2) Finn, C.; Schnittger, S.; Yellowlees, L. J.; Love, J. B. Molecular Approaches to the Electrochemical Reduction of Carbon Dioxide. *Chem. Commun.* **2012**, *48*, 1392−1399.

(3) Jin, S.; Hao, Z.; Zhang, K.; Yan, Z.; Chen, J. Advances and Challenges for the Electrochemical Reduction of CO_2 to CO: From Fundamentals to Industrialization. *Angew. Chem., Int. Ed.* **2021**, *60*, 20627−20648.

(4) Ma, W.; He, X.; Wang, W.; Xie, S.; Zhang, Q.; Wang, Y. Electrocatalytic Reduction of CO_2 and CO to Multi-Carbon Compounds over Cu-Based Catalysts. *Chem. Soc. Rev.* **2021**, *50*, 12897−12914.

(5) Suominen, M.; Kallio, T. What we currently know about Carbon-Supported Metal and Metal Oxide Nanomaterials in Electrochemical CO_2 Reduction. *ChemElectroChem* **2021**, *8*, 2397−2406.

(6) Wang, G.; Chen, J.; Ding, Y.; Cai, P.; Yi, L.; Li, Y.; Tu, C.; Hou, Y.; Wen, Z.; Dai, L. Electrocatalysis for CO_2 Conversion: From Fundamentals to Value-Added Products. *Chem. Soc. Rev.* **2021**, *50*, 4993−5061.

(7) Boutin, E.; Merakeb, L.; Ma, B.; Boudy, B.; Wang, M.; Bonin, J.; Anxolabéhère-Mallart, E.; Robert, M. Molecular Catalysis of CO_2 reduction: Recent Advances and Perspectives in Electrochemical and Light-Driven Processes with Selected Fe, Ni and Co Aza Macrocyclic and Polypyridine Complexes. *Chem. Soc. Rev.* **2020**, *49*, 5772−5809.

(8) Azcarate, I.; Costentin, C.; Robert, M.; Savéant, J.-M. Through-Space Charge Interaction Substituent Effects in Molecular Catalysis Leading to the Design of the Most Efficient Catalyst of CO_2-to-CO Electrochemical Conversion. *J. Am. Chem. Soc.* **2016**, *138*, 16639−16644.

(9) Monti, D.; Ottolina, G.; Carrea, G.; Riva, S. Redox Reactions Catalyzed by Isolated Enzymes. *Chem. Rev.* **2011**, *111*, 4111−4140.

(10) Meneghello, M.; Léger, C.; Fourmond, V. Electrochemical Studies of CO_2-Reducing Metalloenzymes. *Chem. − Eur. J.* **2021**, *27*, 17542−17553.

(11) Svetlitchnyi, V.; Peschel, C.; Acker, G.; Meyer, O. Two Membrane-Associated NiFeS-Carbon Monoxide Dehydrogenases from the Anaerobic Carbon-Monoxide-Utilizing Eubacterium Carboxydothermus Hydrogenoformans. *J. Bacteriol.* **2001**, *183*, 5134−5144.

(12) Hille, R.; Dingwall, S.; Wilcoxen, J. The Aerobic CO Dehydrogenase from Oligotropha Carboxidovorans. *J. Biol. Inorg. Chem.* **2015**, *20*, 243−251.

(13) Can, M.; Armstrong, F. A.; Ragsdale, S. W. Structure, Function, and Mechanism of the Nickel Metalloenzymes, CO Dehydrogenase, and Acetyl-CoA Synthase. *Chem. Rev.* **2014**, *114*, 4149−4174.

(14) Lindahl, P. A. The Ni-Containing Carbon Monoxide Dehydrogenase Family: Light at the End of the Tunnel? *Biochemistry* **2002**, *41*, 2097−2105.
(15) Jeoung, J.-H.; Dobbek, H. Carbon Dioxide Activation at the Ni,Fe-Cluster of Anaerobic Carbon Monoxide Dehydrogenase. *Science* **2007**, *318*, 1461−1464.
(16) Contaldo, U.; Guigliarelli, B.; Perard, J.; Rinaldi, C.; Le Goff, A.; Cavazza, C. Efficient Electrochemical CO_2/CO Interconversion by an Engineered Carbon Monoxide Dehydro-genase on a Gas-Diffusion Carbon Nanotube-Based Bioelectrode. *ACS Catal.* **2021**, *11*, 5808−5817.
(17) Dobbek, H.; Svetlitchnyi, V.; Gremer, L.; Huber, R.; Meyer, O. Crystal Structure of a Carbon Monoxide Dehydrogenase Reveals a Ni-4Fe-5S Cluster. *Science* **2001**, *293*, 1281−1285.
(18) Contaldo, U.; Curtil, M.; Pérard, J.; Cavazza, C.; Le Goff, A. A Pyrene-Triazacyclononane Anchor Affords High Operational Stability for CO_2 RR by a CNT-Supported Histidine-Tagged CODH. *Angew. Chem., Int. Ed.* **2022**, No. e202117212.
(19) Habermüller, K.; Mosbach, M.; Schuhmann, W. Electron-Transfer Mechanisms in Amperometric Biosensors. *Fresenius' J. Anal. Chem.* **2000**, *366*, 560−568.
(20) Shin, W.; Lee, S. H.; Shin, J. W.; Lee, S. P.; Kim, Y. Highly Selective Electrocatalytic Conversion of CO_2 to CO at −0.57 V (NHE) by Carbon Monoxide Dehydrogenase from Moorella Thermoacetica. *J. Am. Chem. Soc.* **2003**, *125*, 14688−14689.
(21) Schuhmann, W.; Wohlschläger, H.; Lammert, R.; Schmidt, H.-L.; Löffler, U.; Wiemhöfer, H.-D.; Göpel, W. Leaching of Dimethylferrocene, a Redox Mediator in Amperometric Enzyme Electrodes. *Sens. Actuators, B* **1990**, *1*, 571−575.
(22) Heller, A. Electron-Conducting Redox Hydrogels: Design, Characteristics and Synthesis. *Curr. Opin. Chem. Biol.* **2006**, *10*, 664−672.
(23) Tapia, C.; Milton, R. D.; Pankratova, G.; Minteer, S. D.; Åkerlund, H.-E.; Leech, D.; De Lacey, A. L.; Pita, M.; Gorton, L. Wiring of Photosystem I and Hydrogenase on an Electrode for Photoelectrochemical H_2 Production by Using Redox Polymers for Relatively Positive Onset Potential. *ChemElectroChem* **2017**, *4*, 90−95.
(24) Yuan, M.; Sahin, S.; Cai, R.; Abdellaoui, S.; Hickey, D. P.; Minteer, S. D.; Milton, R. D. Creating a Low-Potential Redox Polymer for Efficient Electroenzymatic CO_2 Reduction. *Angew. Chem., Int. Ed.* **2018**, *57*, 6582−6586.
(25) So, K.; Sakai, K.; Kano, K. Gas Diffusion Bioelectrodes. *Curr. Opin. Electrochem.* **2017**, *5*, 173−182.
(26) Szczesny, J.; Birrell, J. A.; Conzuelo, F.; Lubitz, W.; Ruff, A.; Schuhmann, W. Redox-Polymer-Based High-Current-Density Gas-Diffusion H_2-Oxidation Bioanode Using FeFe Hydrogenase from Desulfovibrio Desulfuricans in a Membrane-Free Biofuel Cell. *Angew. Chem., Int. Ed.* **2020**, *59*, 16506−16510.
(27) Lielpetere, A.; Becker, J. M.; Szczesny, J.; Conzuelo, F.; Ruff, A.; Birrell, J.; Lubitz, W.; Schuhmann, W. Enhancing the Catalytic Current Response of H_2 Oxidation Gas Diffusion Bioelectrodes Using an Optimized Viologen-Based Redox Polymer and [NiFe] Hydrogenase. *ELSA* **2022**, *2*, No. e2100100.
(28) Ruff, A.; Szczesny, J.; Vega, M.; Zacarias, S.; Matias, P. M.; Gounel, S.; Mano, N.; Pereira, I. A. C.; Schuhmann, W. Redox-Polymer-Wired NiFeSe Hydrogenase Variants with Enhanced O_2 Stability for Triple-Protected High-Current-Density H_2-Oxidation Bioanodes. *ChemSusChem* **2020**, *13*, 3627−3635.
(29) Szczesny, J.; Ruff, A.; Oliveira, A. R.; Pita, M.; Pereira, I. A. C.; de Lacey, A. L.; Schuhmann, W. Electroenzymatic CO_2 Fixation Using Redox Polymer/Enzyme-Modified Gas Diffusion Electrodes. *ACS Energy Lett.* **2020**, *5*, 321−327.
(30) Sehnal, D.; Bittrich, S.; Deshpande, M.; Svobodová, R.; Berka, K.; Bazgier, V.; Velankar, S.; Burley, S. K.; Koča, J.; Rose, A. S. Mol* Viewer: Modern Web App for 3D Visualization and Analysis of Large Biomolecular Structures. *Nucleic Acids Res.* **2021**, *49*, W431−W437.
(31) Dobbek, H.; Svetlitchnyi, V.; Liss, J.; Meyer, O. Carbon Monoxide Induced Decomposition of the Active Site Ni-4Fe-5S Cluster of CO Dehydrogenase. *J. Am. Chem. Soc.* **2004**, *126*, 5382−5387.

https://doi.org/10.1021/acsami.2c09547
ACS Appl. Mater. Interfaces 2022, 14, 46421−46426